

Multi-ring, stripe, and super-lattice solitons in a spin-orbit coupled spin-1 condensate

S. K. Adhikari*

Instituto de Física Teórica, Universidade Estadual Paulista - UNESP, 01.140-070 São Paulo, São Paulo, Brazil

(Dated: January 8, 2021)

We demonstrate exotic stable quasi-two-dimensional solitons in a Rashba or a Dresselhaus spin-orbit (SO) coupled hyperfine spin-1 ($F = 1$) trap-less antiferromagnetic Bose-Einstein condensate using the mean-field Gross-Pitaevskii equation. For weak SO coupling, the solitons are of the $(-1, 0, +1)$ or $(+1, 0, -1)$ type with intrinsic vorticity, for Rashba or Dresselhaus SO coupling, where the numbers in the parentheses denote angular momentum in spin components $F_z = +1, 0, -1$, respectively. For intermediate SO coupling, the solitons have multi-ring structure maintaining the above-mentioned vortices in respective components. For larger SO coupling, *super-lattice* solitons with a square-lattice structure in total density are found in addition to stripe solitons with stripe pattern in component densities with no periodic modulation in total density.

A bright soliton or a soliton is a one-dimensional (1D) shape-preserving solitary wave stabilized by a cancellation of dispersive forces and nonlinear attraction [1]. Quasi-1D solitons have been observed in a Bose-Einstein condensate (BEC) of ${}^7\text{Li}$ [2] and ${}^{85}\text{Rb}$ [3] atoms following a theoretical suggestion [4]. However, solitons cannot be stabilized in two (2D) [5] and three dimensions (3D) [1].

The interest in the creation of spin-orbit (SO) coupling in a BEC increased after the observation of a hyperfine spin-1 spinor BEC of ${}^{23}\text{Na}$ atoms [6]. Although there cannot be a natural SO coupling in a neutral atom, it is possible to introduce an artificial synthetic SO coupling by tuned Raman lasers coupling the different spin states [7, 8]. Two such possible SO couplings are due to Dresselhaus [9] and Rashba [10]. An equal mixture of Dresselhaus and Rashba SO couplings has been experimentally realized in a pseudo spin-1/2 ${}^{87}\text{Rb}$ [11] and ${}^{23}\text{Na}$ [12] BEC of $F_z = 0, -1$ spin states. Later, an SO-coupled spin-1 ${}^{87}\text{Rb}$ BEC of $F_z = \pm 1, 0$ states was observed [13].

A pseudo spin-1/2 SO-coupled BEC can sustain a quasi-1D [14] or a quasi-2D [15] or a 3D [16] soliton. In a spin-1/2 SO-coupled BEC, quantum half-vortex solitons [17] have also been studied and multi-ring and rotating solitons were also found in a periodic potential [18]. Stability of these solitons have also been studied recently [19]. A spin-1 SO-coupled BEC also sustains a quasi-1D [20] or a quasi-2D [21] or a 3D [22] soliton.

Here we undertake a comprehensive study of solitons in a spin-1 quasi-2D Rashba or a Dresselhaus SO-coupled antiferromagnetic BEC. For a weakly Rashba or Dresselhaus SO-coupled spin-1 BEC (SO-coupling strength $\gamma \lesssim 0.75$), the soliton is of the $(\mp 1, 0, \pm 1)$ type of angular momenta $\mp 1, 0, \pm 1$ in components $F_z = +1, 0, -1$ [21, 23], where the positive (negative) sign denotes a vortex (an antivortex) and the upper (lower) sign corresponds to Rashba (Dresselhaus) SO coupling. For medium SO-coupling, we find $(\mp 1, 0, \pm 1)$ -type multi-ring solitons for Rashba or Dresselhaus SO couplings, main-

taining the above-mentioned vortices at the center of respective components. For larger SO-coupling, two types of quasi-degenerate solitons are found. The first type has maxima and minima in density forming a stripe pattern. In the second type, matter is spontaneously distributed on a 2D square lattice. For a Dresselhaus SO-coupled BEC, the density and energy of the solitons are the same as in the case of Rashba coupling, but the two wave functions are different.

The pursuit of a super-solid [24] is a fascinating subject in different areas of condensed matter physics. A super-solid is a quantum state where matter forms a spatially-ordered rigid structure, breaking continuous translational symmetry, as in a crystalline solid, and also enjoys friction-less flow as in a super-fluid, breaking Gauge symmetry. Although, super-solidity was never confirmed in super-fluid helium [25], more recently, it has been suggested [26] and observed [27] in a dipolar BEC. In a spin-1/2 SO-coupled BEC, super-solidity has been realized experimentally [28] in the form of a quasi-1D stripe pattern in density [29–31]. The present solitons with a 2D square-lattice structure in total density [32], viz. Figs. 5(c) and (f) and Fig. 4(f), sharing properties with a conventional supersolid, will be termed super-lattice solitons in the following as suggested in Refs. [29, 32]. The super-lattice solitons are expected to possess coexisting order parameters with super-solid-like properties leading to a periodic spatial structure in total density [29, 32], as illustrated in Fig. 1 of Ref. [32], in Fig. 1 of Ref. [29, 33] and in Fig. 1(e) of Ref. [31, 34]. The multi-ring, viz. Fig. 3, and stripe, viz. Figs. 4(a)-(c), solitons only exhibit a periodic structure in the component densities, due to a phase separation among the components without any periodic structure in the total density. A super-lattice soliton is a unique example of spontaneous 2D crystallization in a free condensed matter system and a study of this may enhance the knowledge about the origin of crystal formation in solids under controlled conditions.

We consider a BEC of N atoms, each of mass m , under a harmonic trap $V(\mathbf{r}) = m\omega_z^2 z^2/2$ of frequency ω_z in the z direction and free in the $x - y$ plane. After integrating out the z coordinate [35], the single particle Hamiltonian

*sk.adhikari@unesp.br

<https://professores.ift.unesp.br/sk.adhikari/>

of the SO-coupled BEC is [11]

$$H_0 = -\frac{\hbar^2}{2m}\nabla_{\boldsymbol{\rho}}^2 + \gamma[\eta p_y \Sigma_x - p_x \Sigma_y], \quad (1)$$

where $\boldsymbol{\rho} \equiv \{x, y\}$, $\nabla_{\boldsymbol{\rho}}^2 = (\partial^2/\partial x^2 + \partial^2/\partial y^2) \equiv (\partial_x^2 + \partial_y^2)$, γ is the strength of the SO-coupling term in square bracket, where $\eta = +1$ for Rashba coupling, $\eta = -1$ for Dresselhaus coupling, and $\eta = 0$ for an equal mixture of Rashba and Dresselhaus couplings, $p_x = -i\hbar\partial_x$, $p_y = -i\hbar\partial_y$ and the spin matrices Σ_x and Σ_y are

$$\Sigma_x = \frac{1}{\sqrt{2}} \begin{pmatrix} 0 & 1 & 0 \\ 1 & 0 & 1 \\ 0 & 1 & 0 \end{pmatrix}, \quad \Sigma_y = \frac{i}{\sqrt{2}} \begin{pmatrix} 0 & -1 & 0 \\ 1 & 0 & -1 \\ 0 & 1 & 0 \end{pmatrix}. \quad (2)$$

A quasi-2D Rashba SO-coupled spin-1 spinor BEC is described by the following set of Gross-Pitaevskii equations [36] at zero temperature for spin components $F_z = \pm 1, 0$ [37, 38]

$$i\partial_t \psi_{\pm 1}(\boldsymbol{\rho}) = [\mathcal{H} + c_2(n_{\pm 1} - n_{\mp 1} + n_0)]\psi_{\pm 1}(\boldsymbol{\rho}) + \{c_2\psi_0^2(\boldsymbol{\rho})\psi_{\mp 1}^*(\boldsymbol{\rho})\} - i\tilde{\gamma}(\eta\partial_y \pm i\partial_x)\psi_0(\boldsymbol{\rho}), \quad (3)$$

$$i\partial_t \psi_0(\boldsymbol{\rho}) = [\mathcal{H} + c_2(n_{+1} + n_{-1})]\psi_0(\boldsymbol{\rho}) + \{2c_2\psi_{+1}(\boldsymbol{\rho}) \times \psi_{-1}(\boldsymbol{\rho})\psi_0^*(\boldsymbol{\rho})\} - i\tilde{\gamma}[-i\partial_x\phi_{-1}(\boldsymbol{\rho}) + \eta\partial_y\phi_{+1}(\boldsymbol{\rho})], \quad (4)$$

$$\mathcal{H} = -\frac{1}{2}\nabla_{\boldsymbol{\rho}}^2 + c_0 n, \quad (5)$$

$$c_0 = \frac{2N\sqrt{2\pi}(a_0 + 2a_2)}{3}, \quad c_2 = \frac{2N\sqrt{2\pi}(a_2 - a_0)}{3}, \quad (6)$$

where $\phi_{\pm 1}(\boldsymbol{\rho}) = \psi_{+1}(\boldsymbol{\rho}) \pm \psi_{-1}(\boldsymbol{\rho})$, $\partial_t \equiv \partial/\partial t$, $\tilde{\gamma} = \gamma/\sqrt{2}$, $n_j = |\psi_j|^2$, $j = \pm 1, 0$ are the densities of spin components $F_z = \pm 1, 0$, and $n(\boldsymbol{\rho}) = \sum_j n_j(\boldsymbol{\rho})$ the total density, a_0 and a_2 are the scattering lengths in the total spin 0 and 2 channels, respectively, and the asterisk denotes complex conjugate. All quantities in Eqs. (3)-(6) and in the following are dimensionless; this is achieved by expressing length (a_0, a_2, x, y, z) in units of oscillator length $l_0 \equiv \sqrt{\hbar/m\omega_z}$, density in units of l_0^{-2} , energy in units of $\hbar\omega_z$, and time in units of ω_z^{-1} . A spin-1 spinor BEC is classified into two magnetic phases [38]: ferromagnetic ($c_2 < 0$) and antiferromagnetic ($c_2 > 0$). The normalization condition is $\int n(\boldsymbol{\rho}) d\boldsymbol{\rho} = 1$. The time-independent version of Eqs. (3)-(4), appropriate for stationary solutions, can be derived from the energy functional

$$E[\psi] = \frac{1}{2} \int d\boldsymbol{\rho} \left\{ \sum_j |\nabla_{\boldsymbol{\rho}} \psi_j|^2 - 2\mu n + c_0 n^2 + c_2 [n_{+1}^2 + n_{-1}^2 + 2(n_{+1}n_0 + n_{-1}n_0 - n_{+1}n_{-1} + \psi_{-1}^*\psi_0^2\psi_{+1}^* + \psi_{-1}\psi_0^2\psi_{+1})] - 2i\tilde{\gamma}[\eta\psi_0^*\partial_y\phi_{+1} + \eta\phi_{+1}^*\partial_y\psi_0 - i\psi_0^*\partial_x\phi_{-1} + i\phi_{-1}^*\partial_x\psi_0] \right\} + \mu, \quad (7)$$

where μ is the chemical potential.

To solve Eqs. (3) and (4) numerically, we propagate these in time by the split-time-step Crank-Nicolson discretization scheme [39] with the boundary condition that

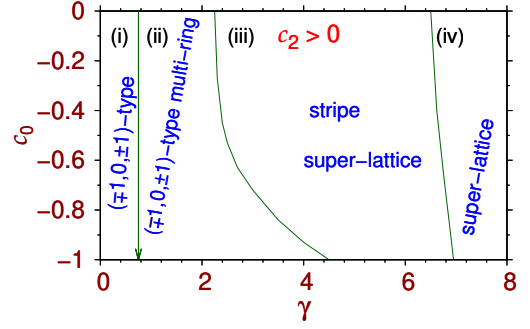


FIG. 1: The c_0 versus γ phase plot showing soliton formation in a Rashba or a Dresselhaus SO-coupled spin-1 antiferromagnetic BEC in different regions of parameter space: formation of (i) $(\mp 1, 0, \pm 1)$ -type, (ii) $(\mp 1, 0, \pm 1)$ -type multi-ring, (iii) stripe, and (iii,iv) super-lattice solitons. The upper (lower) sign correspond to Rashba (Dresselhaus) coupling. Results in all figures are plotted in dimensionless units.

the wave-function components and their first derivatives vanish at the boundary while using a space step of 0.1 and a time step of 0.001 for imaginary-time propagation and 0.00025 for real-time propagation. All calculations of soliton profiles employ imaginary-time approach with the conservation of normalization during time propagation, which finds the lowest-energy solution of each type. Real-time propagation is used to test the stability of the solitons. Magnetization ($= \int d\boldsymbol{\rho} [n_{+1} - n_{-1}]$) is not a good quantum number and is left to freely evolve during time propagation to attain a final converged value consistent with the parameters of the problem. However, this converged value was found to be zero in all cases studied.

We study the formation of a quasi-2D soliton in a self-attractive ($c_0 < 0$) spin-1 antiferromagnetic BEC for different sets of parameters: the nonlinearities c_0, c_2 and SO-coupling strength γ . The scenario of soliton formation for Rashba or Dresselhaus SO coupling is illustrated in the phase plot of c_0 versus γ for $c_2 > 0$ in Fig. 1. Solitons of type $(\mp 1, 0, \pm 1)$ are formed in region (i), whereas $(\mp 1, 0, \pm 1)$ -type multi-ring solitons are formed in region (ii). In region (iii), stripe solitons are formed and super-lattice solitons are possible in regions (iii) and (iv). The phase plot remains unchanged independent of the value of c_2 unless it is too large. No visible change in the phase plot is found for $10 > c_2 > 0$, consistent with an analytical result that the density and energy of a weakly SO-coupled spin-1 BEC soliton are independent of c_2 for quasi-1D [40] and quasi-2D [21] settings. For smaller values of c_0 ($c_0 < -1$), because of an excess of attraction the soliton acquires a small size of the order of the lattice period and the crystalline structure is lost.

First, we consider $(\mp 1, 0, \pm 1)$ -type solitons for small γ ($\gamma \lesssim 0.75$) for Rashba (upper sign) or Dresselhaus (lower sign) SO coupling. In Fig. 2 we display the contour plot of density of components (a) $j = \pm 1$, (b) $j = 0$, and (c) total density of a $(\mp 1, 0, \pm 1)$ -type soliton for parameters

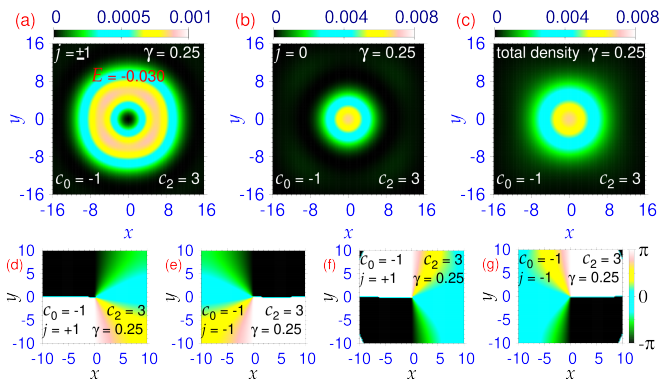


FIG. 2: Contour plot of density n_j of a $(\mp 1, 0, \pm 1)$ -type spin-1 Rashba or Dresselhaus SO-coupled BEC soliton for components (a) $j = \pm 1$, (b) $j = 0$ and (c) total density. The phases of the wave functions of components $j = \pm 1$ of the $(-1, 0, +1)$ -type Rashba SO-coupled soliton shown in (a) are displayed in (d) and (e). The same of components $j = \pm 1$ for a $(+1, 0, -1)$ -type spin-1 Dresselhaus SO-coupled BEC soliton are illustrated in (f) and (g).

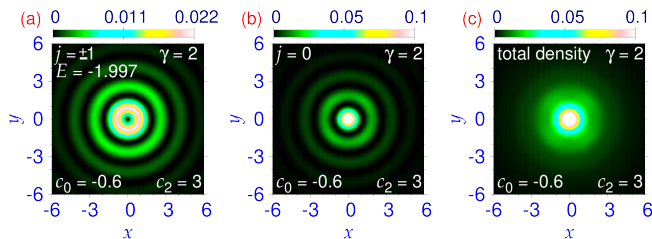


FIG. 3: Contour plot of density n_j of a $(\mp 1, 0, \pm 1)$ -type multi-ring spin-1 Rashba or Dresselhaus SO-coupled BEC soliton for components (a) $j = \pm 1$, (b) $j = 0$ and (c) total density.

$c_0 = -1, c_2 = 3, \gamma = 0.25$. The energy and density of the $(\mp 1, 0, \pm 1)$ -type soliton are insensitive to the variation of c_2 in the range $10 > c_2 > 0$ [21, 40]. The energy of the $(\mp 1, 0, \pm 1)$ -type soliton in Fig. 2 is $E = -0.030$ independent of the type of SO coupling: Rashba or Dresselhaus. In Figs. 2(d)-(e) we display the contour plot of the phase of wave function components $j = \pm 1$ of the $(-1, 0, +1)$ -type Rashba SO-coupled soliton of Fig. 2(a) showing a phase drop of $\mp 2\pi$ under a complete rotation, indicating angular momenta of ∓ 1 in these components. Although the densities for Rashba and Dresselhaus SO-coupled solitons are the same the corresponding phases for Dresselhaus SO-coupling are different, viz. Figs. 2(f)-(g) showing the phases of components $j = \pm 1$ of the Dresselhaus SO-coupled soliton corresponding to a phase drop of $\pm 2\pi$ under a complete rotation, indicating angular momenta of ± 1 in these components. These phases are consistent with the vortex-antivortex structure of the $(\mp 1, 0, \pm 1)$ -type solitons for Rashba and Dresselhaus couplings.

To study multi-ring solitons for medium γ , in Fig. 3 we show the contour plot of density of components (a) $j = \pm 1$ and (b) $j = 0$ and (c) total density of a

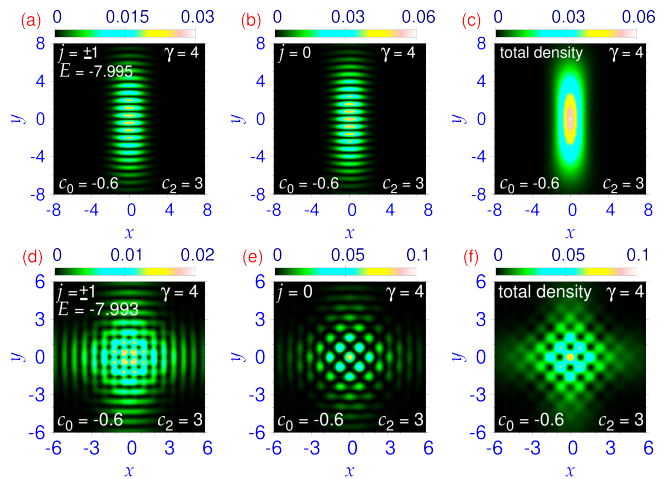


FIG. 4: Contour plot of density n_j of a stripe spin-1 Rashba or Dresselhaus SO-coupled BEC soliton of components (a) $j = \pm 1$ and (b) $j = 0$ (c) the total density. The same of a super-lattice soliton of components (d) $j = \pm 1$, (e) $j = 0$, and (f) the total density.

$(\mp 1, 0, \pm 1)$ -type multi-ring soliton for Rashba or Dresselhaus SO couplings for $c_0 = -0.6, c_2 = 3, \gamma = 2$. Although, there is modulation in density of different components, the total density shows no modulation. The phases in this case (not shown) are identical to the same of the $(\mp 1, 0, \pm 1)$ -type soliton shown in Figs. 2(d)-(g) reflecting the same vortex-antivortex structure at the center of the respective components for Rashba or Dresselhaus SO couplings. The energy of the $(\mp 1, 0, \pm 1)$ -type multi-ring soliton in Fig. 3 is $E = -1.997$ for both SO couplings. The increase of γ from Fig. 2 to Fig. 3 has increased the binding, and hence aids in forming soliton. The change in binding due to the change of c_0 from Fig. 2 to Fig. 3 is negligible in this scale. Multi-ring solitons were also investigated in a quasi-2D pseudo spin-1/2 SO-coupled BEC trapped in a radially periodic potential [18] which creates the multi-ring modulation in density. However, the present radial modulation in density without any external trap is a consequence of the SO couplings.

As γ is increased, the $(\mp 1, 0, \pm 1)$ -type multi-ring solitons continue to exist but will not be considered further. Two new types of solitons *without* any vortex at the center of the components appear as quasidegenerate states: stripe and super-lattice solitons with periodic distribution of matter in x and/or y directions. The single particle Hamiltonian (1) should have solutions of the plane wave form $\exp(\pm i\alpha\gamma x) \otimes \exp(\pm i\beta\gamma y)$, where α and β are constants. In the presence of interaction ($c_0, c_2 \neq 0$), the solution will be a superposition of such plane wave solutions leading to a periodic variation of density in the form $\sin^2(\alpha\gamma x), \cos^2(\beta\gamma y), \sin^2(\alpha\gamma x) \sin^2(\beta\gamma y)$ etc. appropriate for stripe or lattice solitons. This has been demonstrated in details for quasi-1D solitons [20], the same of the present quasi-2D solitons will be the subject of a future investigation. The period of the lattice or stripe

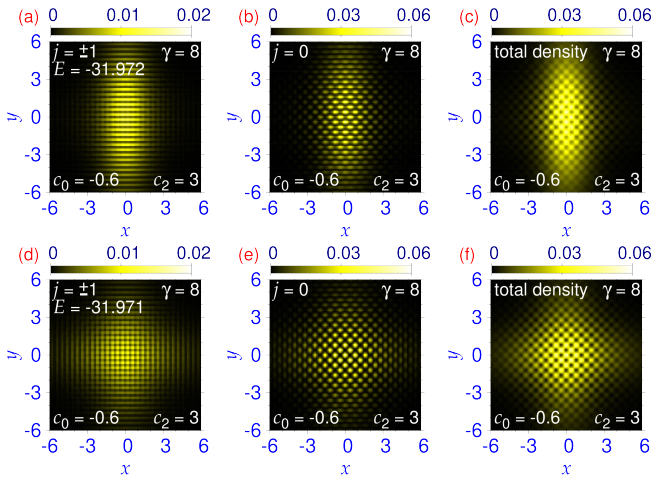


FIG. 5: Contour plot of density n_j of a super-lattice spin-1 Rashba or Dresselhaus SO-coupled BEC soliton (with a periodic stripe in $j = \pm 1$) for components (a) $j = \pm 1$, (b) $j = 0$, and (c) the total density. The same of a super-lattice soliton with a square-lattice pattern in components (d) $j = \pm 1$, (e) $j = 0$, and (f) the total density.

increases as γ is reduced. For small γ , the size of the soliton is smaller than this period and the periodic pattern in density is not possible. In Fig. 4 we illustrate a quasi-2D stripe soliton for $c_0 = -0.6, c_2 = 3$, and $\gamma = 4$ through a contour plot of density of components (a) $j = \pm 1$, (b) $j = 0$, and (c) total density, obtained by imaginary-time propagation using an initial localized wave function modulated by appropriate stripes in form $\sin(\gamma x)$ and $\cos(\gamma x)$ for $j = \pm 1$ and 0 components. Although, there is a stripe pattern in density in this case, the positions of maxima in components $j = \pm 1$ coincide with the minima in component $j = 0$ due to a phase separation among the components, thus resulting in a total density without modulation. In Fig. 4 the super-lattice soliton for the same set of parameters is displayed through a contour plot of density of components (d) $j = \pm 1$, (e) $j = 0$, and (f) total density, obtained by imaginary-time propagation using the converged wave function of Fig. 3 as the initial state. The distribution of matter on a 2D square lattice is prominent in the total density plot of Fig. 4(f) [32]. For the same set of parameters, the stripe soliton of energy $E = -7.995$ and the super-lattice soliton of energy $E = -7.993$ are almost degenerate states with the stripe solitons having slightly smaller energy.

As γ is further increased, the stripe solitons become super-lattice solitons with 2D square-lattice structure in total density. In Fig. 5 we display the contour plot of density of such a super-lattice soliton of components (a) $j = \pm 1$, (b) $j = 0$, (c) total density for parameters $c_0 = -0.6, c_2 = 3$, and $\gamma = 8$. In this case, the component densities of Fig. 5(a) ($j = \pm 1$) continue to possess a 1D stripe pattern but the total density in Fig. 5(c) and the density of the $j = 0$ component in Fig. 5(b) develop a prominent 2D square-lattice structure [32]. The com-

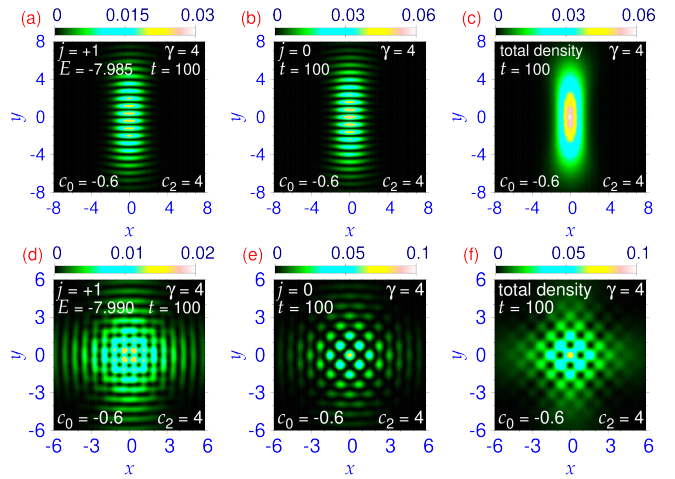


FIG. 6: Contour plot of density of a stripe BEC soliton, of Fig. 4(a)-(c), of components (a) $j = \pm 1$, (b) $j = 0$ and (c) the total density, after real-time propagation at time $t = 100$ upon a change of c_2 from 3 to 4 at $t = 0$. The same of a super-lattice soliton, of Fig. 4(d)-(f), of components (d) $j = \pm 1$, (e) $j = 0$ and (f) the total density.

ponent densities as well as the total density of a super-lattice soliton with 2D square-lattice structure in both are displayed in Fig. 5 for (d) $j = \pm 1$, (e) $j = 0$, and (f) the total density. These two types of super-lattice solitons have practically the same energy: $E = -31.972$ and -31.971 , respectively.

To demonstrate the dynamical stability of the solitons, we consider the stripe and the super-lattice solitons of Fig. 4 and subject the corresponding imaginary-time wave functions to real-time propagation during 100 units of time after changing c_2 from 3 to 4. The resultant density of the stripe soliton is displayed in Fig. 6 for components (a) $j = \pm 1$, (b) $j = 0$, and (c) total density. The same for the super-lattice soliton are shown in Figs. 6(d)-(f). Although the root-mean-square sizes and energy were oscillating (different energies in Figs. 4 and 6) during real-time propagation, the periodic pattern in total density survived at $t = 100$. If the solitons were not dynamically stable, the small numerical deviation due to a change of c_2 from 3 to 4 would have destroyed the periodic pattern in density.

At a finite temperature, there will be a thermal cloud outside the super-fluid soliton and the present study at zero temperature may require corrections [41]. For ultra-low-density scalar BEC solitons [2, 3], the experimental result [42] for the critical number of atoms in a ^{85}Rb soliton at low temperature is in excellent agreement with that derived from the zero-temperature GP equation [43] with an estimated error of less than 1%. As the present solitons are also of ultra-low density with very small $|c_0|$, the finite-temperature corrections in an experiment are expected to be small. Hence we do not believe the finite-temperature correction to be so large as to invalidate the general findings of this study.

In the pseudo spin-1/2 SO-coupled quasi-2D BEC only stripe state was found [31]. In the quasi-2D spin-1 case, in this study, we find both stripe and 2D square lattice states. However, in a quasi-2D spin-1 BEC we could not find any super-lattice state for an equal mixture of Rashba and Dresselhaus couplings, which is a simpler 1D coupling. Preliminary studies indicate that in the quasi-2D spin-2 case there could be formation of stripe, square lattice and hexagonal lattice [44] states. It seems that a more intricate SO coupling with an increased number of wave function components is responsible for a diverse type of super-lattice states.

We demonstrated new types of dynamically stable solitons in a Rashba or Dresselhaus SO-coupled spin-1 quasi-2D untrapped spinor antiferromagnetic ($c_2 > 0$) BEC for medium and large SO-coupling strengths γ . For medium γ , $(\mp 1, 0, \pm 1)$ -type multi-ring solitons are found for Rashba and Dresselhaus SO couplings. As γ is increased, stripe and super-lattice solitons are found, where matter is distributed either in stripe form with maxima and minima or on a square quasi-2D lattice. The to-

tal density of the stripe soliton has no density modulation, whereas that of the super-lattice soliton shows a 2D square lattice pattern, viz. Fig. 4 for $\gamma = 4$. As γ is further increased, the stripe solitons become super-lattice solitons, viz. Figs. 5(a)-(c) for $\gamma = 8$, where the total density exhibits a 2D periodic structure on a square lattice. The spontaneous formation of a 2D square-lattice structure in the total density of super-lattice solitons is remarkable in being a trap-less super-fluid system showing crystallization behavior. These super-lattice solitons are dynamically robust and deserve further theoretical and experimental investigation.

Acknowledgments

The author thanks Dr. Sandeep Gautam and Ms. Prsdeep Kaur for discussion and acknowledges support by the CNPq (Brazil) grant 301324/2019-0, and by the ICTP-SAIFR-FAPESP (Brazil) grant 2016/01343-7

-
- [1] Y. S. Kivshar and B. A. Malomed, *Rev. Mod. Phys.* **61**, 763 (1989); F. K. Abdullaev, A. Gammal, A. M. Kamchatnov, and L. Tomio, *Int. J. Mod. Phys. B* **19**, 3415 (2005).
- [2] K. E. Strecker, G. B. Partridge, A. G. Truscott, and R. G. Hulet, *Nature (London)* **417**, 150 (2002); L. Khaykovich, F. Schreck, G. Ferrari, T. Bourdel, J. Cubizolles, L. D. Carr, Y. Castin, and C. Salomon, *Science* **256**, 1290 (2002).
- [3] S. L. Cornish, S. T. Thompson, and C. E. Wieman, *Phys. Rev. Lett.* **96**, 170401 (2006).
- [4] V. M. Pérez-García, H. Michinel, and H. Herrero, *Phys. Rev. A* **57**, 3837 (1998).
- [5] R. Y. Chiao, E. Garmire, and C. H. Townes, *Phys. Rev. Lett.* **13**, 479 (1964).
- [6] J. Stenger, S. Inouye, D. M. Stamper-Kurn, H.-J. Miesner, A. P. Chikkatur, W. Ketterle, *Nature (London)* **396**, 345 (1998).
- [7] J. Dalibard, F. Gerbier, G. Juzeliunas, P. Öhberg, *Rev. Mod. Phys.* **83**, 1523 (2011).
- [8] V. Galitski and I. B. Spielman, *Nature (London)* **494**, 49 (2013).
- [9] G. Dresselhaus, *Phys. Rev.* **100**, 580 (1955).
- [10] E. I. Rashba, *Fiz. Tverd. Tela* **2**, 1224 (1960); [English Transla.: *Sov. Phys. Solid State* **2**, 1109 (1960).]
- [11] Y.-J. Lin, K. Jiménez-García, I. B. Spielman, *Nature (London)* **471**, 83 (2011).
- [12] J. Li, W. Huang, B. Shteynas, S. Burchesky, F. C. Top, E. Su, J. Lee, A. O. Jamison, and W. Ketterle, *Phys. Rev. Lett.* **117**, 185301 (2016).
- [13] D. Campbell, R. Price, A. Putra, A. Valdés-Curiel, D. Trypogeorgos, and I. B. Spielman, *Nat. Commun.* **7**, 10897 (2016).
- [14] V. Achilleos, D. J. Frantzeskakis, P. G. Kevrekidis, and D. E. Pelinovsky, *Phys. Rev. Lett.* **110**, 264101 (2013).
- [15] H. Sakaguchi, B. Li, and B. A. Malomed, *Phys. Rev. E* **89**, 032920 (2014); H. Sakaguchi and B. A. Malomed, *Phys. Rev. E* **90**, 062922 (2014).
- [16] Y.-C. Zhang, Z.-W. Zhou, B. A. Malomed, and H. Pu, *Phys. Rev. Lett.* **115**, 253902 (2015).
- [17] V. E. Lobanov, Y. V. Kartashov, and V. V. Konotop, *Phys. Rev. Lett.* **112**, 180403 (2014).
- [18] Y. V. Kartashov and D. A. Zezyulin, *Phys. Rev. Lett.* **122**, 123201 (2019).
- [19] Y. V. Kartashov and V. V. Konotop, *Phys. Rev. Lett.* **125**, 054101 (2020).
- [20] S. Gautam and S. K. Adhikari, *Phys. Rev. A* **91**, 063617 (2015).
- [21] S. Gautam and S. K. Adhikari, *Phys. Rev. A* **95**, 013608 (2017).
- [22] S. Gautam and S. K. Adhikari, *Phys. Rev. A* **97**, 013629 (2018).
- [23] T. Mizushima, K. Machida, T. Kita, *Phys. Rev. Lett.* **89**, 030401 (2002); T. Mizushima, K. Machida, T. Kita, *Phys. Rev. A* **66**, 053610 (2002).
- [24] E.P. Gross, *Phys. Rev.* **106**, 161 (1957); A. F. Andreev and I. M. Lifshitz, *Zurn. Eksp. Teor. Fiz.* **56**, 2057 (1969) [English Transla.: *Sov. Phys. JETP* **29**, 1107 (1969)]; A. J. Leggett, *Phys. Rev. Lett.* **25**, 1543 (1970); G. V. Chester, *Phys. Rev. A* **2**, 256 (1970); M. Boninsegni and N. V. Prokof'ev, *Rev. Mod. Phys.* **84**, 759 (2012); V. I. Yukalov, *Phys.* **2**, 49 (2020).
- [25] E. Kim and M. H. W. Chan, *Nature (London)* **427**, 225 (2004); S. Balibar, *Nature (London)* **464**, 176 (2010).
- [26] R. Bombin, J. Boronat, and F. Mazzanti, *Phys. Rev. Lett.* **119**, 250402 (2017); F. Cinti and Massimo Boninsegni, *J. Low Temp. Phys.* **196**, 413 (2019); Zhen-Kai Lu, Yun Li, D. S. Petrov, and G. V. Shlyapnikov, *Phys. Rev. Lett.* **115**, 075303 (2015); N. Y. Yao, C. R. Laumann, A. V. Gorshkov, S. D. Bennett, E. Demler, P. Zoller, and M. D. Lukin *Phys. Rev. Lett.* **109**, 266804 (2012); K. Góral, L. Santos and M. Lewenstein, *Phys. Rev. Lett.* **88**, 170406 (2002); B. Capogrosso-Sansone, C. Trefzger, M. Lewenstein, P. Zoller, and G. Pupillo, *Phys. Rev. Lett.*

- 104**, 125301 (2010).
- [27] F. Böttcher, J.-N. Schmidt, M. Wenzel, J. Hertkorn, M. Guo, T. Langen, and T. Pfau, *Phys. Rev. X* **9**, 011051 (2019); F. Cinti and M. Boninsegni, *J. Low Temp. Phys.* **196**, 413 (2019); J. Hertkorn, F. Böttcher, M. Guo, J. N. Schmidt, T. Langen, H. P. Büchler, and T. Pfau, *Phys. Rev. Lett.* **123**, 193002 (2019); L. Tanzi, E. Lucioni, F. Famà, J. Catani, A. Fioretti, C. Gabbanini, R. N. Bisset, L. Santos, and G. Modugno, *Phys. Rev. Lett.* **122**, 130405 (2019); L. Chomaz, D. Petter, P. Ilzhöfer, G. Natale, A. Trautmann, C. Politi, G. Durastante, R. M. W. van Bijnen, A. Patscheider, M. Sohmen, M. J. Mark, and F. Ferlaino, *Phys. Rev. X* **9**, 021012 (2019); G. Natale, R. M. W. van Bijnen, A. Patscheider, D. Petter, M. J. Mark, L. Chomaz, and F. Ferlaino, *Phys. Rev. Lett.* **123**, 050402 (2019).
- [28] J.-R. Li, J. Lee, W. Huang, S. Burchesky, B. Shteynas, F. Ç. Top, A. O. Jamison, and W. Ketterle, *Nature (London)* **543**, 91 (2017).
- [29] Y. Li, G. I. Martone, L. P. Pitaevskii, and S. Stringari, *Phys. Rev. Lett.* **110**, 235302 (2013).
- [30] T.-L. Ho and S. Zhang, *Phys. Rev. Lett.* **107**, 150403 (2011); R. Liao, *Phys. Rev. Lett.* **120**, 140403 (2018).
- [31] S. Sinha, R. Nath, and L. Santos, *Phys. Rev. Lett.* **107**, 270401 (2011).
- [32] A. Putra, F. Salces-Carcoba, Y. Yue, S. Sugawa, and I. B. Spielman, *Phys. Rev. Lett.* **124**, 053605 (2020).
- [33] In this figure the overlapping in-phase modulations in the spin-up and down components add up to a periodic modulation in total density.
- [34] The name super-solid does not appear in Ref. [31]. The term super-solid in this context was emphasized later in Refs. [29, 32].
- [35] L. Salasnich, A. Parola, L. Reatto, *Phys. Rev. A* **65**, 043614 (2002).
- [36] E. P. Gross, *Nuovo Cim.* **20**, 454 (1961); L.P. Pitaevskii, *Zurn. Eksp. Teor. Fiz.* **40**, 646 (1961)[English Transla.: *Sov. Phys. JETP.* **13**, 451 (1961)].
- [37] V. I. Yukalov, *Laser Phys.* **28**, 053001 (2018); S. Gautam, S. K. Adhikari, *Phys. Rev. A* **92**, 023616 (2015).
- [38] Y. Kawaguchi, M. Ueda, *Phys. Rep.* **520**, 253 (2012).
- [39] R. Ravisankar, D. Vudragović, P. Muruganandam, A. Balaž, and S. K. Adhikari, *Comput. Phys. Commun.* **259**, 107657 (2021); P. Muruganandam and S. K. Adhikari, *Comput. Phys. Commun.* **180**, 1888 (2009); D. Vudragović, I. Vidanović, A. Balaž, P. Muruganandam, S. K. Adhikari, *Comput. Phys. Commun.* **183**, 2021 (2012); L. E. Young-S., P. Muruganandam, S. K. Adhikari, V. Lončar, D. Vudragović, A. Balaž, *Comput. Phys. Commun.* **220**, 503 (2017).
- [40] S. Gautam and S. K. Adhikari, *Laser Phys. Lett.* **12**, 045501 (2015).
- [41] F. Dalfovo, S. Giorgini, L. P. Pitaevskii, and S. Stringari, *Rev. Mod. Phys.* **71**, 463 (1999).
- [42] N. R. Claussen, S. J. J. M. F. Kokkelmans, S. T. Thompson, E. A. Donley, E. Hodby, and C. E. Wieman, *Phys. Rev. A* **67**, 060701(R) (2003).
- [43] A. Gammal, T. Frederico, and L. Tomio, *Phys. Rev. A* **64**, 055602 (2001).
- [44] S. Gautam and S. K. Adhikari, unpublished.